

Room-temperature operation of hot-electron transistors

A. F. J. Levi

AT&T Bell Laboratories, Murray Hill, New Jersey 07974

T. H. Chiu

AT&T Bell Laboratories, Holmdel, New Jersey 07733

(Received 18 May 1987; accepted for publication 31 July 1987)

We demonstrate the first room-temperature operation of a double heterojunction unipolar hot-electron transistor. Our test structure has a current gain greater than 10 and a measured current drive capability in excess of 1200 A cm^{-2} . The device uses an indirect, wide-band-gap $\text{AlSb}_{0.92}\text{As}_{0.08}$ emitter and the transistor base is a 100-\AA -wide InAs layer.

There are similarities between a unipolar hot-electron transistor (HET) and an n - p - n double heterojunction bipolar transistor. Both, for example, have high current drive capability. However, in contrast to the bipolar, for a given geometry, the unipolar HET has a very low base resistance R_b due to the high electron (compared to hole) mobility. In principle, the unipolar also has low forward bias emitter-base capacitance C_{eb} due to the absence of minority-carrier diffusion effects. Hence, the $R_b C_{eb}$ time constant limiting bipolar speed is unimportant in a suitably designed unipolar HET allowing the possibility that ultimate device speed depends only upon the hot-electron emitter-collector transit time. Consequently, there is interest in developing unipolar HET's for high-speed electronics applications.¹⁻³

In this letter we report progress fabricating a unipolar HET in the AlGaInAsSb material system lattice matched to GaSb. Figure 1 shows a schematic band diagram of the device under bias. The use of a wide-band-gap $\text{AlSb}_{0.92}\text{As}_{0.08}$ emitter allows room-temperature operation because, unlike previous HET's, electrons are injected approximately 1.3 eV above the conduction-band minimum of the base which is more than 50 times greater than ambient thermal energies of around 0.025 eV . The transistor base consists of a 100-\AA -thick epilayer of InAs with a carrier concentration of two dimensionally confined electrons, $n \sim 2 \times 10^{12} \text{ cm}^{-2}$. The confinement energy E_0 of these electrons serves to increase the effective band gap of InAs while retaining the advantage of the semiconductor's low effective electron mass. The collector arm is 3500 \AA of unintentionally doped GaSb and the entire epilayer structure was grown by molecular beam epitaxy on a (001) oriented n -type GaSb substrate. The crystal growth techniques we used are essentially similar to those described in Ref. 4. The lattice mismatch of 6×10^{-3} between InAs and GaSb is accommodated by elastic deformation of the InAs lattice in the narrow base region. This elastic deformation modifies the valence-band structure in a known way⁵ but has little effect on the conduction band and so for the purpose of the present discussion its effect is ignored. After removal from the growth chamber the wafer was fabricated into a two-level mesa structure allowing emitter, base, and collector to be contacted individually and the device characteristics measured. Special mention should be made concerning contact to the transistor base. This is achieved using the natural electron accumulation layer oc-

curing at the exposed InAs surface. We use a 400-\AA -thick AuGe alloy for contact metallization and the alloy is annealed for a few seconds at $230 \text{ }^\circ\text{C}$ in a hydrogen atmosphere. Following this, Ti/Au metallization is deposited and samples are bonded onto standard 16-pin packages for convenient electrical characterization.

In Figs. 2(a) and 2(b) typical measured common base current gain α and common emitter current gain β are shown for a device maintained at a temperature of 300 K . Although there is good agreement between the α and β measurements, the saturation characteristics are nonideal exhibiting a small slope with increasing collector voltage bias. As may be seen in Fig. 2(b), the room-temperature value of β increases from $\beta = 10$ at $V_{ce} = 1.0 \text{ V}$ to $\beta = 17$ at $V_{ce} = 3.0 \text{ V}$. At liquid-nitrogen temperature $\beta = 12$ at $V_{ce} = 1.0 \text{ V}$ and $\beta = 40$ at $V_{ce} = 3.0 \text{ V}$. We note that the reduction in base/collector potential barrier, ϕ_{bc} , with increasing collector voltage bias, V_{ce} , improves collector efficiency for incoming hot electrons and, in agreement with simple calculations, contributes to the observed slope in the common emitter saturation characteristics. In addition, useful analysis of emitter, base, and collector current in different biasing configurations reveals that ionization by hot carriers in the collector is unimportant for low values of V_{ce} but dominates the gain characteristics for $V_{ce} \gtrsim 4.0 \text{ V}$. We therefore obtain a

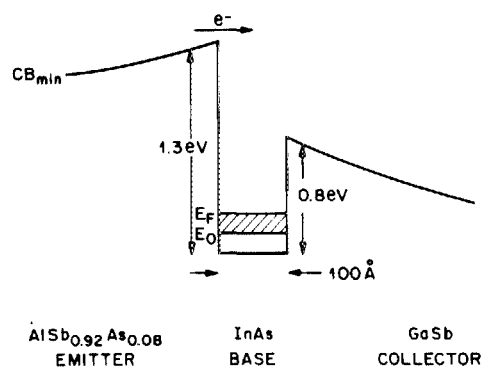


FIG. 1. Schematic diagram of the conduction band of an $\text{AlSb}_{0.92}\text{As}_{0.08}/\text{InAs}/\text{GaSb}$ double heterojunction unipolar HET under bias. The conduction-band minimum CB_{min} is indicated as the confinement energy E_0 and the Fermi energy E_F of the occupied two-dimensional electron states in the InAs base.

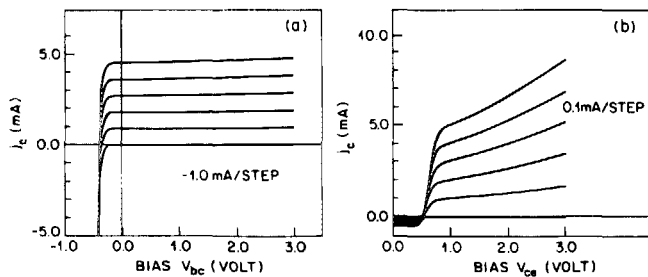


FIG. 2. (a) Room-temperature (300 K) common base current gain characteristics of the device shown schematically in Fig. 1. Curves were taken in steps of -1.0 mA beginning with an injected emitter current of zero. (b) Room-temperature common emitter current gain characteristics of the device in (a). Curves were taken in steps of 0.1 mA beginning with an injected base current of zero.

lower limit for current gain in the transistor by measuring β at a bias just above threshold, $V_{ce} \sim 1.0$ V. Using this criterion and to confirm the high current drive capability of the device we have measured $\beta = 10$ for collected current of less than 1 to 100 mA (corresponding to current densities from less than 10 to more than 1200 A cm^{-2}).

To gain deeper insight into the physics determining performance of this unipolar HET it is necessary to consider details such as the kinematic and dynamical constraints imposed on hot-electron transport in the device. Consider a thermal electron injected from a state close to the X minimum of the $\text{AlSb}_{0.92}\text{As}_{0.08}$ conduction band into a high-energy Γ state in the InAs base. Because, in the absence of scattering, the injection process conserves energy and momentum parallel to the interface, band structure considerations dictate that electrons cannot be injected into large parallel momentum states. The injected electrons therefore traverse the base in the minimum possible time with a large component of momentum perpendicular to the interface. The kinematic constraints giving rise to this type of injection window only occur at certain heterojunction interfaces. In Fig. 3 we illustrate the kinematics of an electron of energy E_i traversing the device by showing the states in the band structure⁶ the electron occupies in the emitter, base, and collector. Once in the base, the injected electron may either be quantum mechanically reflected at the collector barrier, ϕ_{bc} , scattered in the base, or traverse the base to contribute to the collected current j_c .

Quantum reflections from ϕ_{bc} can limit device perfor-

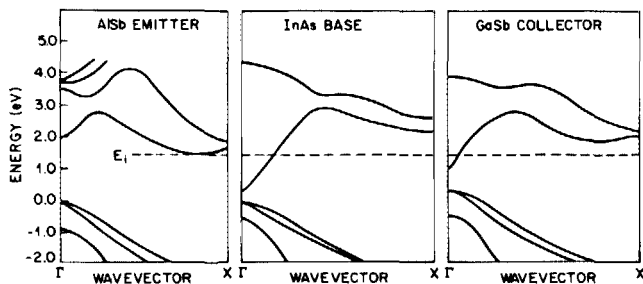


FIG. 3. Band diagrams illustrating the states used in (001) transmission of an electron of energy E_i through an $\text{AlSb}/\text{InAs}/\text{GaSb}$ double heterostructure unipolar HET.

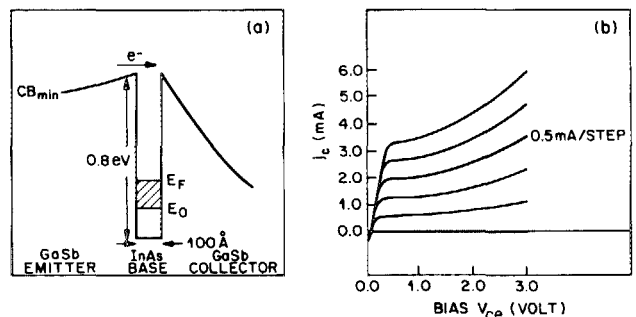


FIG. 4. (a) Schematic diagram of the conduction band of a symmetric $\text{GaSb}/\text{InAs}/\text{GaSb}$ double heterojunction unipolar HET under bias. (b) Room-temperature common emitter current gain of the device shown schematically in (a). Curves were taken in steps of 0.5 mA beginning with an injected base current of zero.

mance. A dramatic illustration of the role played by these reflections is obtained by replacing the $\text{AlSb}_{0.92}\text{As}_{0.08}$ emitter with GaSb as illustrated in Fig. 4(a). The measured common emitter current gain of such a symmetric device is shown in Fig. 4(b). As may be seen, near threshold β is around 1.3 corresponding to more than 43% of injected electrons being trapped in the base region and contributing to base current. However, quantum reflections are not a *fundamental* limit to device performance. Using the established boundary conditions employed in the effective mass approximation⁷ it is straightforward to show that reflections from the abrupt change in potential at ϕ_{bc} approach zero when the hot-electron velocity (in general $\partial\omega/\partial k$ at E_i) is the same either side of the base-collector junction. This impedance matching condition is $m_1/m_2 = E_i/(E_i - \phi_{bc})$, where m_1 and m_2 are the effective electron masses in the base and collector, respectively. Hence, by choosing E_i , ϕ_{bc} , base, and collector materials, including the possible use of superlattices, quantum reflections from ϕ_{bc} can be eliminated.

It is known that hot-electron scattering rates in the base present a fundamental limit to device performance.¹ Unfortunately, there are difficulties in estimating the importance of this dynamical constraint in the present device as we are unable to distinguish base current arising from inelastic scattering and that due to quantum reflection at ϕ_{bc} . In addition, a satisfactory theory which describes scattering rates for perpendicular transport across a two-dimensional electron gas has yet to be formulated. We note that any such theory must address two competing effects: first, the reduction, compared to the three-dimensional case, in screening which will tend to increase scattering rates and second, the small scattering angles, typical of Coulomb scattering, which will tend to decrease scattering rates for perpendicular transport. Clearly, a theoretical understanding of the relative importance of these processes would be useful.

In conclusion, we have demonstrated room-temperature operation of a double heterojunction unipolar transistor with high current drive capability and common emitter current gain greater than 10. This was achieved using a wide-band-gap $\text{AlSb}_{0.92}\text{As}_{0.08}$ emitter and a 100 -Å-wide InAs base. In addition, our work establishes the electrical quality of the AlGaInAsSb material system and suggests that in the

future potentially useful devices such as HET's, field effect and bipolar transistors may be fabricated from epilayers of AlGaInAsSb lattice matched to GaSb.

We wish to thank D. R. Hamann, R. J. Malik, P. M. Platzman, and S. Schmitt-Rink for useful discussions, M. Anzlower for technical assistance, and R. C. Dynes, H. L. Störmer, and W. T. Tsang for support and encouragement during the course of this project.

¹A. F. J. Levi, J. R. Hayes, and R. Bhat, Appl. Phys. **48**, 1690 (1986); **49**, 1312 (1986), also J. R. Hayes and A. F. J. Levi, IEEE J. Quantum Electron. **22**, 1744 (1986).

²K. Imamura, S. Muto, T. Fujii, N. Yokoyama, S. Hizamizu, and A. Shibamoto, Electron. Lett. **22**, 1148 (1986).

³M. Heiblum, I. M. Anderson, and C. M. Knoedler, Appl. Phys. Lett. **49**, 207 (1986).

⁴W. T. Tsang, T. H. Chiu, D. W. Kisker, and J. A. Ditzenberger, Appl. Phys. Lett. **46**, 283 (1985), also T. H. Chiu, W. T. Tsang, and A. F. J. Levi Electron. Lett. **17**, 917 (1987).

⁵F. H. Pollak, Surf. Sci. **37**, 863 (1973); Y. C. Chang, H. Y. Chu, and S. G. Chung, Phys. Rev. B **33**, 7364 (1986); E. P. O'Reilly and G. P. Witchlow, Phys. Rev. B **34**, 6030 (1986).

⁶Band structures taken from the *Landolt-Bornstein Tables*, edited by O. Madelung, H. Schulz, and H. Weiss (Springer, Berlin, 1982), Vol. III/17a and references therein.

⁷See, for example, Y. Ando and T. Itoh, J. Appl. Phys. **61**, 1497 (1987).